

## On Uncertainty in Global Terrestrial Evapotranspiration Estimates from Choice of Input Forcing Datasets\*

GRAYSON BADGLEY

*Department of Global Ecology, Carnegie Institution for Science, Stanford, California*

JOSHUA B. FISHER

*Jet Propulsion Laboratory, California Institute of Technology, Pasadena, California*

CARLOS JIMÉNEZ

*Laboratoire d'Études du Rayonnement et de la Matière en Astrophysique, Centre National de la Recherche Scientifique, Observatoire de Paris, Paris, France*

KEVIN P. TU

*Theiss Research, Davis, California*

RAGHUVeer VINUKOLLU

*Swiss Re, Armonk, New York*

(Manuscript received 28 February 2014, in final form 17 January 2015)

### ABSTRACT

Evapotranspiration ET is a critical water, energy, and climate variable, and recent work has been published comparing different global products. These comparisons have been difficult to interpret, however, because in most studies the evapotranspiration products were derived from models forced by different input data. Some studies have analyzed the uncertainty in regional evapotranspiration estimates from choice of forcings. Still others have analyzed how multiple models vary with choice of net radiation forcing data. However, no analysis has been conducted to determine the uncertainty in global evapotranspiration estimates attributable to each class of input forcing datasets. Here, one of these models [Priestly–Taylor JPL (PT-JPL)] is run with 19 different combinations of forcing data. These data include three net radiation products (SRB, CERES, and ISCCP), three meteorological datasets [CRU, Atmospheric Infrared Sounder (AIRS) *Aqua*, and MERRA], and three vegetation index products [MODIS; Global Inventory Modeling and Mapping Studies (GIMMS); and Fourier-Adjusted, Sensor and Solar Zenith Angle Corrected, Interpolated, Reconstructed (FASIR)]. The choice in forcing data produces an average range in global monthly evapotranspiration of  $10.6 \text{ W m}^{-2}$  ( $\sim 20\%$  of global mean evapotranspiration), with net radiation driving the majority of the difference. Annual average terrestrial ET varied by an average of  $8 \text{ W m}^{-2}$ , depending on choice of forcings. The analysis shows that the greatest disagreement between input forcings arises from choice of net radiation dataset. In particular, ISCCP data, which are frequently used in global studies, differed widely from the other radiation products examined and resulted in dramatically different estimates of global terrestrial ET.

### 1. Introduction

\* Supplemental information related to this paper is available at the Journals Online website: <http://dx.doi.org/10.1175/JHM-D-14-0040.s1>.

Corresponding author address: Grayson Badgley, Department of Global Ecology, Carnegie Institution for Science, 260 Panama St., Stanford, CA 94305.  
E-mail: badgley@stanford.edu

Evapotranspiration ET is a key variable of the global water budget and is central to agriculture and water management, the spatial distribution of ecosystems, and atmospheric–terrestrial carbon exchanges (Brubaker and Entekhabi 1996; Prentice et al. 1992; Sellers et al. 1996). ET has historically been the most difficult aspect

of the water balance to measure (Lettenmaier and Famiglietti 2006). Studies of trends in ET at continental and watershed scales show little agreement, which has spurred vigorous debate over long-term patterns in global ET (Teuling et al. 2009), with some arguing the trend in global ET is declining (Peterson et al. 1995; Jung et al. 2010) and others finding the opposite (Brutsaert 2006; Wetherald and Manabe 2002). Resolving this issue, however, has been hampered by shortcomings in long-term hydrological datasets (e.g., Peel and McMahon 2006).

Part of this uncertainty stems from the diversity of models and inputs that go into those models used for estimating ET at the global scale. Global, remote sensing-driven, physically derived ET retrieval algorithms require three broad categories of inputs: net radiation, meteorology (e.g., water vapor pressure, air temperature, and wind), and vegetation [e.g., land cover, vegetation greenness indices, and leaf area index (LAI)] (e.g., Fisher et al. 2008; Mu et al. 2007, 2011). As the number and diversity of these input datasets increase, the question emerges as to how differences in input datasets contribute to variability in global ET estimates (Wang and Dickinson 2012).

Two recent studies examined global estimates of ET generated from 41 models of varying complexity, each forced with nonuniform input datasets (Jiménez et al. 2011; Mueller et al. 2011). To advance these efforts, Vinukollu et al. (2011) forced three ET models with the same driving datasets to isolate uncertainty arising from ET models, independent of input data. While they found some major discrepancies in net radiation forcing data, their work suggested that internal model uncertainty surpasses the uncertainty due to the choice of net radiation data. Ferguson et al. (2010) employed a full-ensemble approach to test the sensitivity of evapotranspiration estimates based on choice of emissivity, albedo, vegetation [e.g., normalized difference vegetation index (NDVI) and LAI], and meteorological input data over the continental United States, demonstrating that varying air temperature and vegetation indices forcings introduced the greatest uncertainty, though net radiation data also contributed to the uncertainty of ET estimates. More recently, Mueller and Seneviratne (2014) reported a wide range of ET estimates when comparing output from an array of climate models participating in phase 5 of the Coupled Model Intercomparison Project (CMIP5). These studies have laid the foundation for better quantifying the variability in current estimates of global ET over land.

Here, we build on that foundation by forcing the Priestly–Taylor Jet Propulsion Laboratory (PT-JPL) global ET model (Fisher et al. 2008) with a matrix of input datasets made up of three meteorological datasets, three vegetation index datasets, and three net radiation datasets, resulting in 19 different ET estimates, spanning 1984–2006, though no single product covers the entire

period. To our knowledge, no study has comprehensively explored the global uncertainty attributable to these three classes of forcings in unison. From this experiment, we hope to accomplish three objectives. The first is to quantify the annual variability in global ET estimates over land that results from choice of input dataset. The second is to quantify the variability in ET estimates attributable to each category of input dataset. Finally, we hope to highlight the importance of accounting for differences in forcing datasets when comparing between models, as products can differ in ways that easily mask the real differences in how models function. The performance of ISCCP-based ET estimates within our evaluation framework will serve to illustrate this point.

## 2. Data and methods

Our results are derived from a 23-yr (1984–2006) record of globally gridded 1° ET estimates, calculated using the PT-JPL ET model and driven with monthly input datasets of monthly average net radiation, monthly average daily maximum air temperature, monthly average water vapor pressure, and monthly average NDVI. PT-JPL explicitly partitions ET into soil evaporation, canopy transpiration, and interception evaporation. The model reduces Priestly–Taylor (Priestley and Taylor 1972) potential ET to actual ET through a series of ecophysiological constraint functions. For example, surface wetness is determined without the need of precipitation data and instead relies on a transformation of relative humidity RH<sup>4</sup>, which captures temporal changes in surface wetness (Fisher et al. 2008). The model can be driven entirely with remote sensing and does not include or require calibration, spinup, or initialization.<sup>1</sup> For one class of products, those based on AIRS meteorological data, we substitute daily mean air temperature for daily maximum air temperature (see Armanios and Fisher 2014). We calculated terrestrial ET globally for ice-free land, as defined by Friedl et al. (2010).

For each radiation dataset, we calculated total-sky net radiation. We used a fully satellite-based radiation product from NASA's Clouds and the Earth's Radiant Energy System (CERES) monthly average AVG of the Synoptic Radiative Fluxes and Cloud dataset, using data derived from the tuned total-sky algorithm, calculated using Flight Models 1 and 2 (FM1 and FM2; version 2C) data from the *Terra* sensor. From the International Satellite Cloud Climatology Project (ISCCP), we used the climatological summary product [flux data from surface radiative flux (FD-SRF); available online at see <http://isccp.giss.nasa.gov/projects/flux.html>] dataset regredded

<sup>1</sup> Model code is available at <http://josh.yosh.org/>.

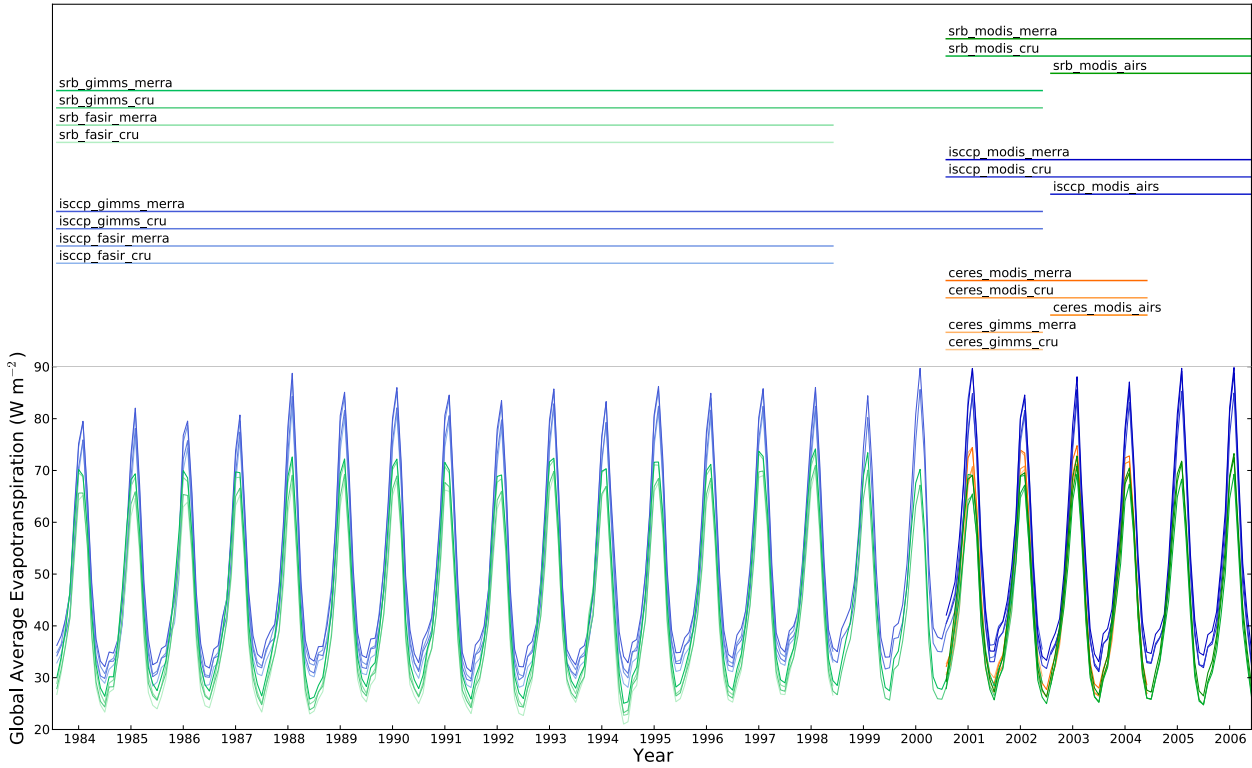


FIG. 1. Monthly, globally averaged terrestrial ET estimates for the 19 possible combinations of driving datasets, given data availability constraints. Each record is colored according to the net radiation product used to calculate ET. The horizontal lines represent the data-combination availability within the long-term record (at the time of writing), denoting the temporal coverage of each ET product.

to  $1^{\circ}$  (Zhang et al. 2004). The final net radiation dataset came from the NASA/Global Energy and Water Cycle Experiment (GEWEX) Surface Radiation Budget (SRB) quality check, release 3.0, globally gridded  $1^{\circ}$  dataset (Stackhouse et al. 2000).

For meteorological data, we used globally gridded station monthly average daily maximum air temperature and monthly average water vapor pressure data from the Climatic Research Unit (CRU) time series, version 3.0 (Mitchell and Jones 2005). We regridded the CRU data from its native resolution of  $0.5^{\circ}$  to  $1^{\circ}$  to correspond to the other input datasets. We also used meteorological data from the Modern-Era Retrospective Analysis for Research and Applications (MERRA) product from NASA's Global Modeling and Assimilation Office (GMAO). We extracted minimum, maximum, and mean air temperature from the "temperature at two meters above displacement height" T2M variable within the diurnal Incremental Analysis Update (IAU) 2D atmospheric single-level diagnostics dataset. We then calculated saturated vapor pressure according to Shuttleworth (1992) and relative humidity using minimum daily air temperature (Lawrence 2005), the same filling technique used in the CRU record (New et al. 2000). We calculated RH from MERRA 2D data to ensure consistency with 2D temperature data. We

regridded the data to  $1^{\circ}$  from MERRA's native resolution of  $0.5^{\circ} \times 0.66^{\circ}$ . Finally, we calculated mean monthly air temperature and monthly average relative humidity data from the Atmospheric Infrared Sounder (AIRS) *Aqua* Level 3 Monthly Gridded Retrieval Product (AIRX3STM), version 5. We linearly interpolated between the two layers straddling surface pressure to calculate surface temperature and relative humidity (see Armanios and Fisher 2014).

Of the three NDVI products, two derived from the Advanced Very High Resolution Radiometer (AVHRR) record and one, spanning a shorter period, derived from the Moderate Resolution Imaging Spectroradiometer (MODIS) instrument. From the AVHRR record, we used the Fourier-Adjusted Sensor and Solar Zenith Angle Corrected, Interpolated, Reconstructed (FASIR) adjusted NDVI product at  $1^{\circ}$  (Los et al. 2000) and the Global Inventory Modeling and Mapping Studies (GIMMS) dataset (Pinzon et al. 2005; Tucker et al. 2005). From MODIS, we used the MOD13C2, version 5, NDVI product, regridded from  $0.05^{\circ}$  to  $1^{\circ}$ .

### 3. Results

We constructed a time series of global average ET for ice-free land spanning 1984–2006 for the possible ensemble

TABLE 1. Number of ensemble members calculated for each year.

Year	Ensemble members
1984	8
1985	8
1986	8
1987	8
1988	8
1989	8
1990	8
1991	8
1992	8
1993	8
1994	8
1995	8
1996	8
1997	8
1998	8
1999	4
2000	4
2001	12
2002	12
2003	9
2004	9
2005	6
2006	6

members of input datasets at the monthly time step ([Fig. 1](#)). Note that the number of products available for comparison changes from year to year ([Table 1](#)). The range of global average ET flux across all available products at the monthly time scale ranged between 21.0 and 90.0  $\text{W m}^{-2}$ , with a 23-yr monthly mean of 46.2  $\text{W m}^{-2}$  across all available ET combinations. The monthly average range between all estimates was 10.6  $\text{W m}^{-2}$ , which represents 23% of the monthly mean. Differences were greatest during the 3-month period of June–August.

Differences between the ET estimates were primarily driven by choice of net radiation. ISCCP-based ET estimates were on average 6.4  $\text{W m}^{-2}$  greater than SRB-based estimates and 6.8  $\text{W m}^{-2}$  greater than CERES-based estimates. Estimates driven by MERRA meteorological data had, on average, higher ET than CRU- and AIRS-based estimates by 3.2 and 1.7  $\text{W m}^{-2}$ , respectively. Estimates of ET using MODIS were higher than those derived from AVHRR GIMMS and FASIR. The combination that resulted in the highest ET estimates was ISCCP-MODIS-MERRA, and the combination that resulted in the lowest ET estimates was SRB-FASIR-CRU. All comparisons between estimates only consider data over the same time period. In general, the ordering of products in terms of magnitude of ET is preserved from month to month.

To attribute variation in ET estimates to each category of input dataset (radiation, temperature, and NDVI), we calculated the difference between pairs of

ET estimates that shared two input datasets (e.g., radiation and vegetation) but differed in the third (to continue the example, meteorology) for the years 2001 and 2002. Using the absolute value of the maximum difference observed, we calculated the maximum variation caused by each category of input dataset ([Fig. 2](#)). As suggested in [Fig. 1](#), net radiation inputs produced the largest range, resulting in differences in monthly global average ET between 3.7 and 26.1  $\text{W m}^{-2}$ . Notably, excluding ISCCP greatly reduced the variability from net radiation to between 0.1 and 1.8  $\text{W m}^{-2}$ . Switching between vegetation indices had a smaller effect than net radiation with ISCCP, producing differences of 0.3 and 2.3  $\text{W m}^{-2}$ . Meteorological inputs caused similar variation, with differences between 0.2 and 1.8  $\text{W m}^{-2}$ . When excluding ISCCP, uncertainty attributable to meteorological and vegetation products often exceeds uncertainty associated with radiation data. Examining the differences between each type of input dataset (e.g., the difference between MODIS and GIMMS NDVI products) provides insight into what causes the differences in modeled ET ([Figs. 1–4](#) in the supplemental materials). For example, ISCCP data produce relatively high net radiation values during the summer months, especially in the tropics. As a result, the largest differences between estimates occur during tropical wet-season months over humid tropical forests (e.g., the Amazon; not shown). Vegetation and meteorological products have their greatest differences across northern latitudes.

The global annual average ET across all products spans a considerable range ([Fig. 3](#)). Global average ET estimates in 2001, for example, differ by up to 17  $\text{W m}^{-2}$ . Estimates of annual global average ET span a range of over 8  $\text{W m}^{-2}$  for the typical year, depending on the choice of forcing products. When compared over common timespans, ET estimates can offer conflicting information about multiyear changes in global average ET. The SRB-FASIR-MERRA and SRB-GIMMS-CRU, for example, showed no trend over the periods for which data were available. From 1984 to 2006, ISCCP-GIMMS-MERRA shows a slight increase in global annual ET of 0.1  $\text{W m}^{-2} \text{yr}^{-1}$  ( $p < 0.05$ ; single-tailed Student's  $t$  test). This same effect can be seen at shorter time scales. SRB-based estimates decline from 1999 to 2000, while ISCCP-based estimates increase ([Fig. 1](#)).

#### 4. Discussion

The variability in ET estimates is related to differences between input datasets and the unique sensitivities of ET models. In this study, we isolate the uncertainty resulting from inputs to the PT-JPL model. It comes as no surprise that PT-JPL, which derives from

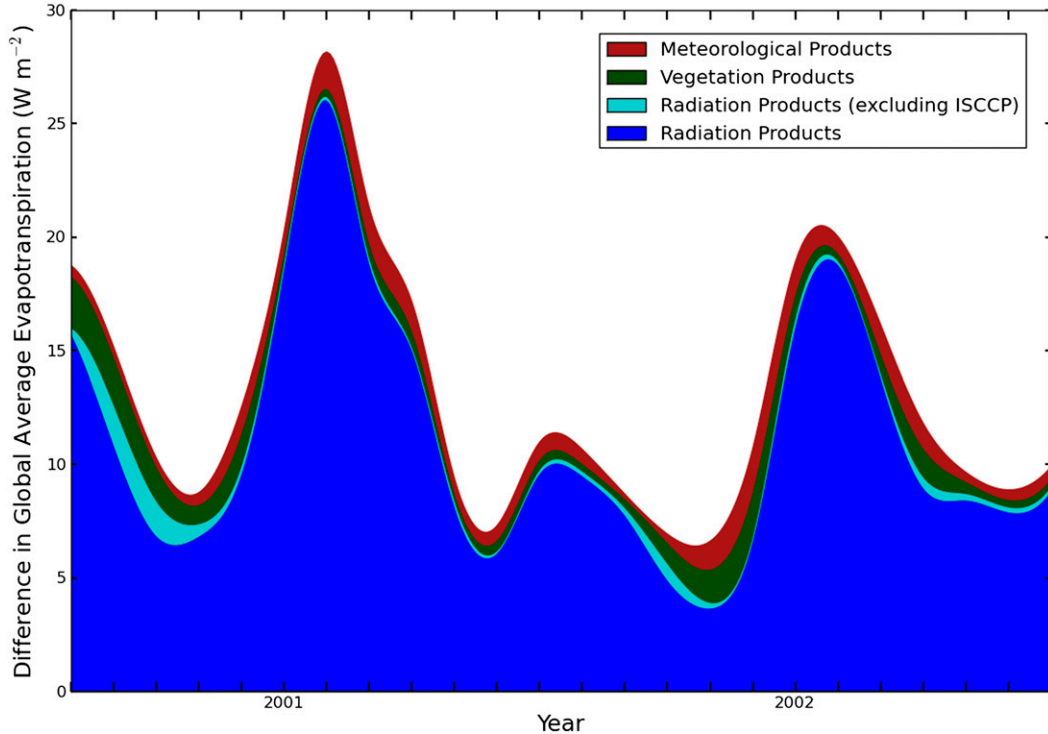


FIG. 2. Absolute value of difference between ET estimates attributable to each type of input dataset, evaluated for the years 2001 and 2002. AIRS data are not included in the meteorological datasets evaluated here.

Priestly–Taylor, is most sensitive to net radiation inputs (Fisher et al. 2008). Rather than confirming this well-established point, our results underscore how the variation across global net radiation products constitutes an appreciable source of uncertainty in estimating global ET on land. For all years in which ISCCP data were available, 60.4% of the monthly average range in estimates of global average ET was attributable to the ISCCP dataset. This large difference must be kept in mind when performing intercomparisons where various net radiation products are used. Vinukollu et al. (2011) identified step changes in the long-term record of ISCCP data and chose to exclude it from their analysis. If we exclude ISCCP from our results, the uncertainty attributable to net radiation inputs falls below the uncertainty associated with choice of vegetation index and comparable to the uncertainty attributable to atmospheric inputs. This is despite the sensitivity of PT-JPL to net radiation inputs, highlighting the ongoing need to resolve the disagreement between forcing datasets that are often used and compared across in the literature (see also Fig. 1 in the supplemental materials). Our initial work here suggests that ISCCP might not be well suited for use with PT-JPL when estimating terrestrial ET at the global scale.

The high degree of variability of estimates of global terrestrial ET within a single month underscores the

difficulty of determining if global average ET has increased or decreased over the past decades (Fig. 3). Our results suggest that determining which forcing datasets are valid for this type of global analysis is a key part of the challenge. Picking among the monthly estimates of global terrestrial ET across all products available in a single month varied by an average of  $10.6 \text{ W m}^{-2}$ , roughly 20% of global mean ET (Fig. 1). Differences in both the sign and magnitude of changes in global annual ET when forced with varying input datasets highlights the uncertainty surrounding the ongoing debate over conflicting long-term trends in global ET (Teuling et al. 2009). Changes in algorithms, the underlying quality of data, and the time periods covered by the ET products we generated for this study prevent us from weighing in on this debate. Instead, our work provides a quantitative example of the appreciable disagreements, especially in estimates of net radiation between commonly used forcing datasets, yet to be overcome.

The meteorological and vegetation input datasets contributed less to the overall uncertainty of ET estimates, accounting for variations of less than  $2.5 \text{ W m}^{-2}$ . This close agreement is especially encouraging given that the input datasets come from a variety of sources, such as remote sensing, model outputs, reanalysis products, and ground-station data. It hints at the possibility of creating a long-term, calibrated ET dataset from

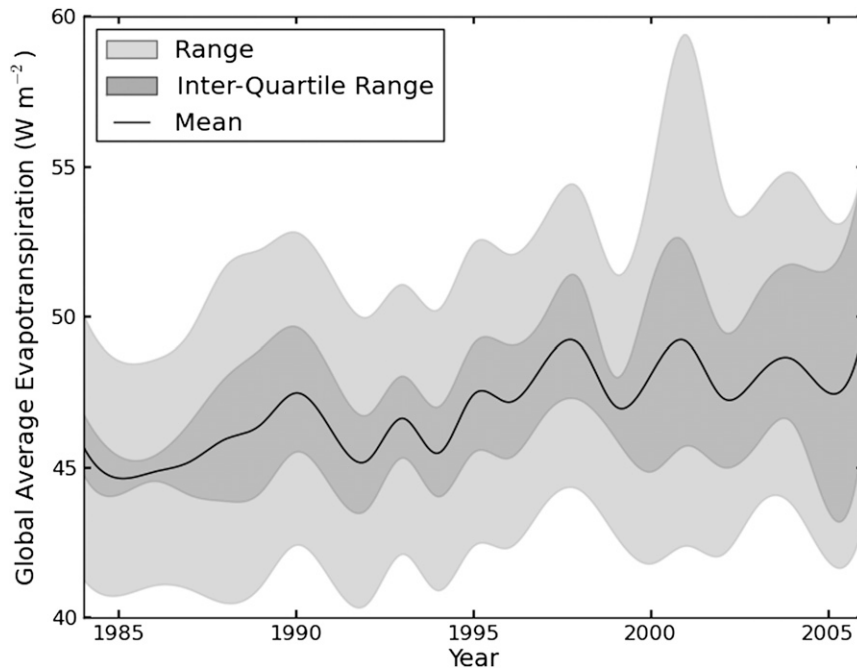


FIG. 3. The range, interquartile range, and mean of annual average ET, calculated from 19 possible combinations of input datasets. The black line represents the mean of all ET estimates for an individual year. All values were smoothed using a univariate-spline function.

heterogeneous sources, though this work would require finer-resolution analysis of both regional and seasonal trends in evapotranspiration. But as our results demonstrate, remotely sensed estimates of surface net radiation are still fraught with uncertainties (Kandel 2012), a limitation that must be overcome if we hope to have reliable estimates of global terrestrial evapotranspiration. Recent work by Pan et al. (2012) shows the promise of fusing data from multiple sources to produce high-quality, long-term records of ET over land.

Keeping these possibilities in mind, it is important to stress that the results of this study rely on a single dedicated ET model, when other ET models exist. Recent ET model intercomparisons have shown a considerable range, up to  $\sim 25 \text{ W m}^{-2}$ , in ET estimates across ET models (Jiménez et al. 2011; Mueller et al. 2011), even when those models are forced with identical driving datasets (Vinukollu et al. 2011). Our work here demonstrates the importance of also considering uncertainty in input datasets, advancing similar efforts previously performed at the regional scale (Ferguson et al. 2010). This previous work, combined with the findings presented here, illustrates the need for a full-ensemble approach for evaluating global ET estimates, where multiple global ET models are forced with a unified matrix of input datasets. While our work revealed interesting characteristics about the PT-JPL model, this approach should prove even more useful when applied to multiple models, in

an attempt to untangle individual model eccentricities from variations introduced from input datasets. When combined with ground truth observations, this line of inquiry promises to improve our ability to model ET at the global scale through further refinement of existing models by isolating, and then minimizing, sources of uncertainty in ET estimates.

**Acknowledgments.** We thank the Global Modeling and Assimilation Office (GMAO) and the GES DISC for the dissemination of MERRA. MODIS data were distributed by the Land Processes Distributed Active Archive Center (LP DAAC), located at the U.S. Geological Survey (USGS) Earth Resources Observation and Science (EROS) Center ([lpdaac.usgs.gov](http://lpdaac.usgs.gov)). CERES data were obtained from the NASA Langley Research Center Atmospheric Science Data Center. A special thanks to T. Troy and E. Wood for providing ISCCP and SRB net radiation data. D. Armanios assisted in processing the AIRS data. M. Jung and M. McCabe provided helpful reviews. Funding was provided by NASA's Terrestrial Hydrology Program and by JPL's Research and Technology Development Strategic Climate and Water Initiatives. The research described in this paper was carried out by the Jet Propulsion Laboratory, California Institute of Technology, under a contract with the National Aeronautics and Space Administration. Government sponsorship acknowledged.

## REFERENCES

- Armanios, D. E., and J. B. Fisher, 2014: Measuring water availability with limited ground data: Assessing the feasibility of an entirely remote-sensing-based hydrologic budget of the Rufiji basin, Tanzania, using TRMM, GRACE, MODIS, SRB, and AIRS. *Hydrol. Processes*, **28**, 853–867, doi:[10.1002/hyp.9611](https://doi.org/10.1002/hyp.9611).
- Brubaker, K. L., and D. Entekhabi, 1996: Analysis of feedback mechanisms in land–atmosphere interaction. *Water Resour. Res.*, **32**, 1343–1357, doi:[10.1029/96WR00005](https://doi.org/10.1029/96WR00005).
- Brutsaert, W., 2006: Indications of increasing land surface evaporation during the second half of the 20th century. *Geophys. Res. Lett.*, **33**, L20403, doi:[10.1029/2006GL027532](https://doi.org/10.1029/2006GL027532).
- Ferguson, C. R., J. Sheffield, E. F. Wood, and H. Gao, 2010: Quantifying uncertainty in a remote sensing–based estimate of evapotranspiration over continental USA. *Int. J. Remote Sens.*, **31**, 3821–3865, doi:[10.1080/01431161.2010.483490](https://doi.org/10.1080/01431161.2010.483490).
- Fisher, J. B., K. P. Tu, and D. D. Baldocchi, 2008: Global estimates of the land–atmosphere water flux based on monthly AVHRR and ISLSCP-II data, validated at 16 FLUXNET sites. *Remote Sens. Environ.*, **112**, 901–919, doi:[10.1016/j.rse.2007.06.025](https://doi.org/10.1016/j.rse.2007.06.025).
- Friedl, M. A., D. Sulla-Menashe, B. Tan, A. Schneider, N. Ramankutty, A. Sibley, and X. Huang, 2010: MODIS Collection 5 global land cover: Algorithm refinements and characterization of new datasets. *Remote Sens. Environ.*, **114**, 168–182, doi:[10.1016/j.rse.2009.08.016](https://doi.org/10.1016/j.rse.2009.08.016).
- Jiménez, C., and Coauthors, 2011: Global intercomparison of 12 land surface heat flux estimates. *J. Geophys. Res.*, **116**, D02102, doi:[10.1029/2010JD014545](https://doi.org/10.1029/2010JD014545).
- Jung, M., and Coauthors, 2010: Recent decline in the global land evapotranspiration trend due to limited moisture supply. *Nature*, **467**, 951–954, doi:[10.1038/nature09396](https://doi.org/10.1038/nature09396).
- Kandel, R., 2012: Understanding and measuring Earth's energy budget: From Fourier, Humboldt, and Tyndall to CERES and beyond. *Surv. Geophys.*, **33**, 337–350, doi:[10.1007/s10712-011-9162-y](https://doi.org/10.1007/s10712-011-9162-y).
- Lawrence, M. G., 2005: The relationship between relative humidity and the dewpoint temperature in moist air: A simple conversion and applications. *Bull. Amer. Meteor. Soc.*, **86**, 225–233, doi:[10.1175/BAMS-86-2-225](https://doi.org/10.1175/BAMS-86-2-225).
- Lettenmaier, D. P., and J. S. Famiglietti, 2006: Hydrology: Water from on high. *Nature*, **444**, 562–563, doi:[10.1038/444562a](https://doi.org/10.1038/444562a).
- Los, S. O., and Coauthors, 2000: A global 9-yr biophysical land surface dataset from NOAA AVHRR data. *J. Hydrometeorol.*, **1**, 183–199, doi:[10.1175/1525-7541\(2000\)001<0183:AGYBLS>2.0.CO;2](https://doi.org/10.1175/1525-7541(2000)001<0183:AGYBLS>2.0.CO;2).
- Mitchell, T. D., and P. D. Jones, 2005: An improved method of constructing a database of monthly climate observations and associated high-resolution grids. *Int. J. Climatol.*, **25**, 693–712, doi:[10.1002/joc.1181](https://doi.org/10.1002/joc.1181).
- Mu, Q., F. A. Heinsch, M. Zhao, and S. W. Running, 2007: Development of a global evapotranspiration algorithm based on MODIS and global meteorology data. *Remote Sens. Environ.*, **111**, 519–536, doi:[10.1016/j.rse.2007.04.015](https://doi.org/10.1016/j.rse.2007.04.015).
- , M. Zhao, and S. W. Running, 2011: Improvements to a MODIS global terrestrial evapotranspiration algorithm. *Remote Sens. Environ.*, **115**, 1781–1800, doi:[10.1016/j.rse.2011.02.019](https://doi.org/10.1016/j.rse.2011.02.019).
- Mueller, B., and S. I. Seneviratne, 2014: Systematic land climate and evapotranspiration biases in CMIP5 simulations. *Geophys. Res. Lett.*, **41**, 128–134, doi:[10.1002/2013GL058055](https://doi.org/10.1002/2013GL058055).
- , and Coauthors, 2011: Evaluation of global observations–based evapotranspiration datasets and IPCC AR4 simulations. *Geophys. Res. Lett.*, **38**, L06402, doi:[10.1029/2010GL046230](https://doi.org/10.1029/2010GL046230).
- New, M., M. Hulme, and P. Jones, 2000: Representing twentieth-century space–time climate variability. Part II: Development of 1901–96 monthly grids of terrestrial surface climate. *J. Climate*, **13**, 2217–2238, doi:[10.1175/1520-0442\(2000\)013<2217:RTCSTC>2.0.CO;2](https://doi.org/10.1175/1520-0442(2000)013<2217:RTCSTC>2.0.CO;2).
- Pan, M., A. K. Sahoo, T. J. Troy, R. K. Vinukollu, J. Sheffield, and E. F. Wood, 2012: Multisource estimation of long-term terrestrial water budget for major global river basins. *J. Climate*, **25**, 3191–3206, doi:[10.1175/JCLI-D-11-00300.1](https://doi.org/10.1175/JCLI-D-11-00300.1).
- Peel, M. C., and T. A. McMahon, 2006: Continental runoff: A quality-controlled global runoff data set. *Nature*, **444**, E14, doi:[10.1038/nature05480](https://doi.org/10.1038/nature05480).
- Peterson, T., V. Golubev, and P. Ya. Groisman, 1995: Evaporation is losing its strength. *Nature*, **377**, 687–688, doi:[10.1038/377687b0](https://doi.org/10.1038/377687b0).
- Pinzon, J., M. E. Brown, and C. J. Tucker, 2005: EMD correction of orbital drift artifacts in satellite data stream. *Hilbert-Huang Transform and Its Applications*, N. E. Huang and S. S. Shen, Eds., World Scientific, 167–186.
- Prentice, I., and Coauthors, 1992: A global biome model based on plant physiology and dominance, soil properties and climate. *J. Biogeogr.*, **19**, 117–134, doi:[10.2307/2845499](https://doi.org/10.2307/2845499).
- Priestley, C. H. B., and R. J. Taylor, 1972: On the assessment of surface heat flux and evaporation using large-scale parameters. *Mon. Wea. Rev.*, **100**, 81–92, doi:[10.1175/1520-0493\(1972\)100<0081:OTAOSH>2.3.CO;2](https://doi.org/10.1175/1520-0493(1972)100<0081:OTAOSH>2.3.CO;2).
- Sellers, P. J., and Coauthors, 1996: Comparison of radiative and physiological effects of doubled atmospheric CO<sub>2</sub> on climate. *Science*, **271**, 1402–1406, doi:[10.1126/science.271.5254.1402](https://doi.org/10.1126/science.271.5254.1402).
- Shuttleworth, J. W., 1992: Evaporation. *Handbook of Hydrology*, D. R. Maidment, Ed., McGraw-Hill, 4.1–4.53.
- Stackhouse, P. W., S. K. Gupta, S. J. Cox, M. Chiacchio, and J. C. Mikovitz, 2000: The WCRP/GEWEX Surface Radiation Budget Project Release 2: An assessment of surface fluxes at 1 degree resolution. *Current Problems in Atmospheric Radiation: Proc. Int. Radiation Symp.*, St. Petersburg, Russia, International Radiation Symposium.
- Teuling, A. J., and Coauthors, 2009: A regional perspective on trends in continental evaporation. *Geophys. Res. Lett.*, **36**, L02404, doi:[10.1029/2008GL036584](https://doi.org/10.1029/2008GL036584).
- Tucker, C. J., J. E. Pinzon, M. E. Brown, D. Slayback, E. W. Pak, R. Mahoney, E. Vermote, and N. El Saleous, 2005: An extended AVHRR 8-km NDVI data set compatible with MODIS and SPOT vegetation NDVI data. *Int. J. Remote Sens.*, **26**, 4485–5598, doi:[10.1080/01431160500168686](https://doi.org/10.1080/01431160500168686).
- Vinukollu, R. K., R. Meynadier, J. Sheffield, and E. F. Wood, 2011: Multi-model, multi-sensor estimates of global evapotranspiration: Climatology, uncertainties and trends. *Hydrol. Processes*, **25**, 3993–4010, doi:[10.1002/hyp.8393](https://doi.org/10.1002/hyp.8393).
- Wang, K., and R. E. Dickinson, 2012: A review of global terrestrial evapotranspiration: Observation, modeling, climatology, and climatic variability. *Rev. Geophys.*, **50**, RG2005, doi:[10.1029/2011RG000373](https://doi.org/10.1029/2011RG000373).
- Wetherald, R. T., and S. Manabe, 2002: Simulation of hydrologic changes associated with global warming. *J. Geophys. Res.*, **107**, 4379, doi:[10.1029/2001JD001195](https://doi.org/10.1029/2001JD001195).
- Zhang, Y. C., W. B. Rossow, A. A. Lacis, V. Oinas, and M. I. Mishchenko, 2004: Calculation of radiative fluxes from the surface to top of atmosphere based on ISCCP and other global data sets: Refinements of the radiative transfer model and the input data. *J. Geophys. Res.*, **109**, D19105, doi:[10.1029/2003JD004457](https://doi.org/10.1029/2003JD004457).